



Late Holocene activity of the Dead Sea Transform revealed in 3D palaeoseismic trenches on the Jordan Gorge segment

Shmuel Marco^{a,*}, Thomas K. Rockwell^b, Ariel Heimann^c,
Uri Frieslander^d, Amotz Agnon^e

^a*Department of Geophysics and Planetary Sciences, Tel Aviv University, Tel Aviv, 69978 Israel*

^b*San Diego State University, California, United States*

^c*The Geological Survey of Israel, Jerusalem, Israel*

^d*The Geophysical Institute of Israel, Lod, Israel*

^e*The Hebrew University, Jerusalem, Israel*

Received 4 May 2004; received in revised form 16 January 2005; accepted 18 January 2005

Available online 20 April 2005

Editor: E. Bard

Abstract

Three-dimensional excavations of buried stream channels that have been displaced by the Jordan Fault, the primary strand of the Dead Sea fault zone in northern Israel, demonstrate that late Holocene slip has been primarily strike-slip at a minimum rate of 3 mm/yr. The palaeoseismic study was carried out in the Bet-Zayda Valley, the delta of the Jordan River at the north shore of the Sea of Galilee. The site was chosen where a north-striking scarp with up to 1-m vertical expression crosses the flat valley. One group of trench excavations was located where a small stream crosses the scarp. The active stream, which is incised into the scarp, is not offset by the fault. However we found two palaeo channels about 2 m below the surface offset sinistrally 2.7 ± 0.2 m by the fault and two younger nested channels offset 0.5 ± 0.05 m. Based on radiocarbon dates we attribute the last 0.5 m rupture to the earthquake of October 30, 1759. The older offset of 2.2 m most probably occurred in the earthquakes of May 20, 1202. These two events correlate with the findings at Ateret, about 12 km north of Bet-Zayda, where the 1202 earthquake produced 1.6 m of lateral displacement in E–W-striking defence walls of a Crusader castle, and an Ottoman mosque was offset 0.5 m in the earthquake of 1759. In the second group of trenches some 60 m farther south we found another offset channel. Its northern margin is displaced 15 m sinistrally whereas the southern margin shows only 9 m of sinistral offset. The dip slip component is 1.2 m, west side down. The different amounts of margin offset can be explained by erosion of the southern margin during the first 6 m of displacement. Additional slip of 9 m accrued after the stream had been abandoned and buried by a 2-m-thick lacustrine clay layers. Radiocarbon dates on organic residue provide the age control which indicates that the 15 m of slip has accrued over the past 5 kyr, yielding a short-term slip rate of 3 mm/yr for the late Holocene. It is possible that our study

* Corresponding author. Tel.: +972 3 6407379; fax: +972 3 6409282.

E-mail address: shmulik@terra.tau.ac.il (S. Marco).

covers only part of the fault zone, hence we regard this mean slip rate to be a minimum for the DST. Based on other palaeoseismic studies the best estimate for Quaternary slip rate is 4 ± 1 mm/yr.

© 2005 Elsevier B.V. All rights reserved.

Keywords: earthquakes; Palaeoseismology; Dead Sea fault; Holocene

1. Introduction

Basic data required for the characterization of seismic activity include the magnitudes and recurrence times of the large earthquakes, the time of the last event on each segment, and the amount of slip in each of the latest earthquakes. In addition to understanding the earthquake phenomenon, this characterization is essential for the assessment of seismic hazard. We began to recover geological data on seismic activity of the Jordan Gorge Fault, a segment of the Dead Sea Transform (DST). The DST accommodates sinistral motion between the Arabia and the Sinai tectonic plates, transferring the opening at the Red Sea to the Taurus–Zagros collision zone (Fig. 1). The paradigm of left-lateral shear along the DST since the Middle Miocene explains the systematic offset of numerous pre-Miocene geologic features by a total of 105 km [1, 2]. It is also consistent with palaeoseismic and archaeoseismic observations [3–6], and with earthquake focal plane solutions [7–9]. Our study was conducted at the Jordan Gorge fault segment, which connects two pull-apart basins in northern Israel, the Sea of Galilee (“Kinneret” in Hebrew) and the Hula valley (Fig. 1). A previous archaeoseismic study determined that E–W trending walls of the Vadum Iacob (Ateret) Crusader fortress, which was built across the Jordan Gorge fault, are offset left-laterally 2.15 ± 0.05 m. An Ottoman mosque, which was built on top of the fortress, is displaced by 0.5 ± 0.05 m [10]. About 1.6 m of the offset was attributed to the large earthquake of 20 May 1202 while the mosque was displaced in the earthquake of 30 October 1759 [3]. These well-dated displacements occurred over a time interval too short to yield meaningful slip rate. The pre-1202 slip event in the study area is also uncertain. Furthermore, geologic mapping and aerial photograph analysis of the Ateret site indicate the presence of another lineament, possibly a fault strand, which does not cross the Ateret structure. Thus the slip determinations on the castle and mosque structures are

minimums for slip in both of these earthquakes at this site, as well as for estimating longer-term slip rates.

The southern end of the Jordan Gorge segment is the basin of the Kinneret, a fault-bounded complex graben [11,12]. The activity in the area is characterized by both strike-slip and normal faulting. Geophysical data from the Kinneret, including seismic imaging [12], gravity [11], and magnetic field [13] do not show a fault along the projected line of the JGF south of the Bet-Zayda. This can be explained by the Jordan delta sediments masking the geophysical signature of the fault, or by the fault terminating just south of the northern lakeshore. In contrast to a single major fault north of the Kinneret, geological mapping and seismic reflections show that there are two active faults south of it [12,14].

2. Trenching investigations

In order to expand our knowledge of the northern part of the DST we searched for a suitable site that can yield a longer earthquake record and impose better constraints on the slip in the historical earthquakes and on the mean slip rate. We hereby report the results of a palaeoseismic trench study in the Jordan fan-delta at the Bet-Zayda Valley (also called “Beteiha”) some 12 km south of Ateret (Fig. 1), near Tel Bet-Zayda, where the miracle of the fish and loaves happened according to Christian tradition. We identified several indicators for a fault and potential slip markers: a lineament co-linear with the Jordan Gorge fault is visible on Landsat 5 images and on air photos (Fig. 2). The lineament is formed by a north-striking scarp, with up to 1 m of vertical expression, which crosses the flat valley. A major fault is observed in deep seismic reflection at the same location [15]. Because the location of the fault at the surface cannot be determined precisely on the deep seismic reflection profile, and in order to examine the width of the fault zone and the number of fault strands near the surface

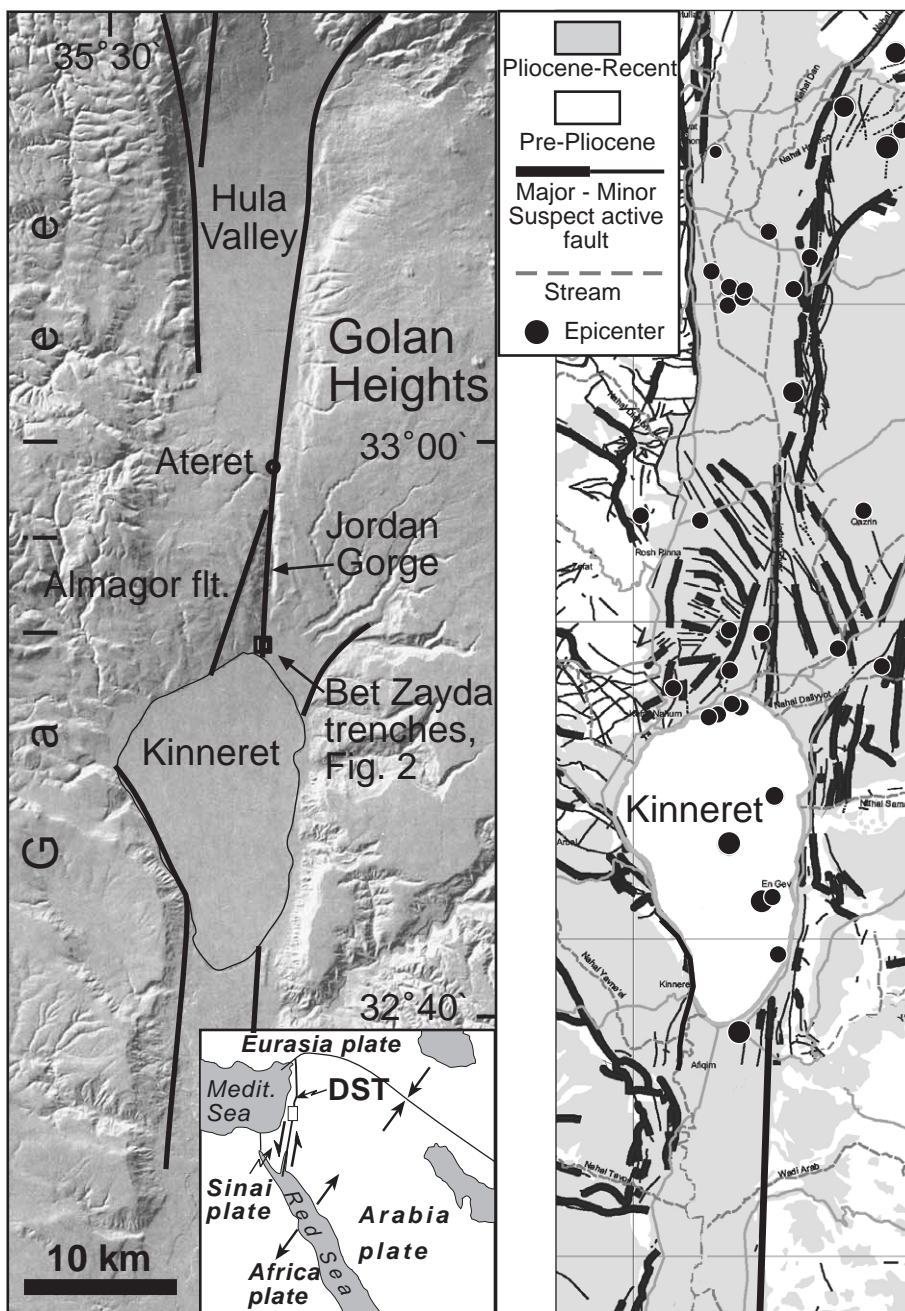


Fig. 1. Left panel: shaded relief and major faults of the Dead Sea Transform system in northern Israel, after [11,45]. Shaded relief by Hall [46]. Inset: tectonic plates in the Middle East. Right panel: map of suspect active faults, after [47].

we performed a high-resolution seismic reflection survey across the valley. Offsets of shallow reflectors are clearly seen on this seismic image (Fig. 3). A stream channel that crosses the scarp from east to west

is not affected by faulting (Fig. 2) but it was a clue for deeper and older streams suitable for measurements of slip. The palaeochannels at this site were the target of our trench study.

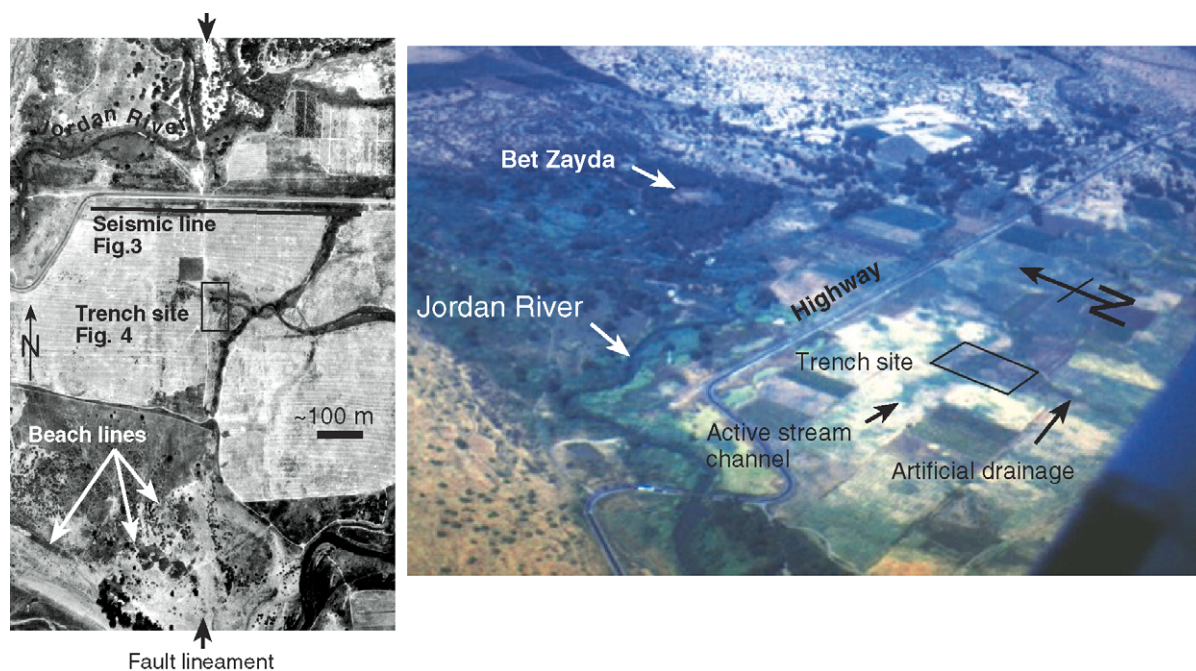


Fig. 2. Left panel: a vertical air photo showing the trench site and location of high-resolution seismic profile (Fig. 3). In addition to the main fault lineament a few other faint N-striking lineaments are noticeable, some of which may be former agricultural elements. Right panel: an oblique air photo of the study area.

2.1. Strategy

The trench site (Figs. 4 and 5) was developed during 3 seasons because the area is cultivated and the trenches had to be filled back at the end of every season. In order to be able to return to exactly the same trench walls we laid nylon sheets of different color for each season before filling the dirt back. We then were able to return in the following year with utmost accuracy.

The first trench, T1, was aimed at confirming the location of the fault. It was dug across the highest part of the scarp, and indeed exposed a clear fault truncating a layer of coarse fluvial sand. This sand layer was observed only on the upthrown (eastern) side. Realizing the fluvial nature of the sand layer, we later opened a series of trenches, called “Southern Trenches”, in order to trace the margins of the sand and delineate the alluvial channel.

Trench 2 was the first in the “Northern Trenches” group. It was located in the middle of the stream channel that crosses the scarp some 60 m north of T1, across the projected line of the scarp. Since the channel is incised into the scarp we expected to find

here channel deposits overlying the fault and post-dating the last faulting event. We also anticipated lower and older channels that may have been offset by the penultimate and perhaps even earlier events. The fault was indeed found at the bottom of T2, offsetting vertically by about 20 cm a layer of channel deposits containing mostly coarse pebbles. Alternating fluvial and lacustrine layers overlay the fault. We subsequently dug two fault-parallel (N-striking) trenches at both ends of T2 in order in search for the channel margins. The margins on the east were found some 2.7 ± 0.3 m north of the margins on the west. Subsequently we excavated additional fault-parallel trenches approaching the fault from both sides until the uncertainty was minimized. Trench 3 was dug approximately half way between T1 and T2 in order to obtain additional points on the fault trace. In T3 we encountered massive dark-brown clayey soil with carbonate concretions cut by a 1-m-wide fault zone. The fault zone is characterized by abundant shear planes, and vertically-smearred carbonate concretions. The sand layer that we saw in T1 was missing in T3, indicating

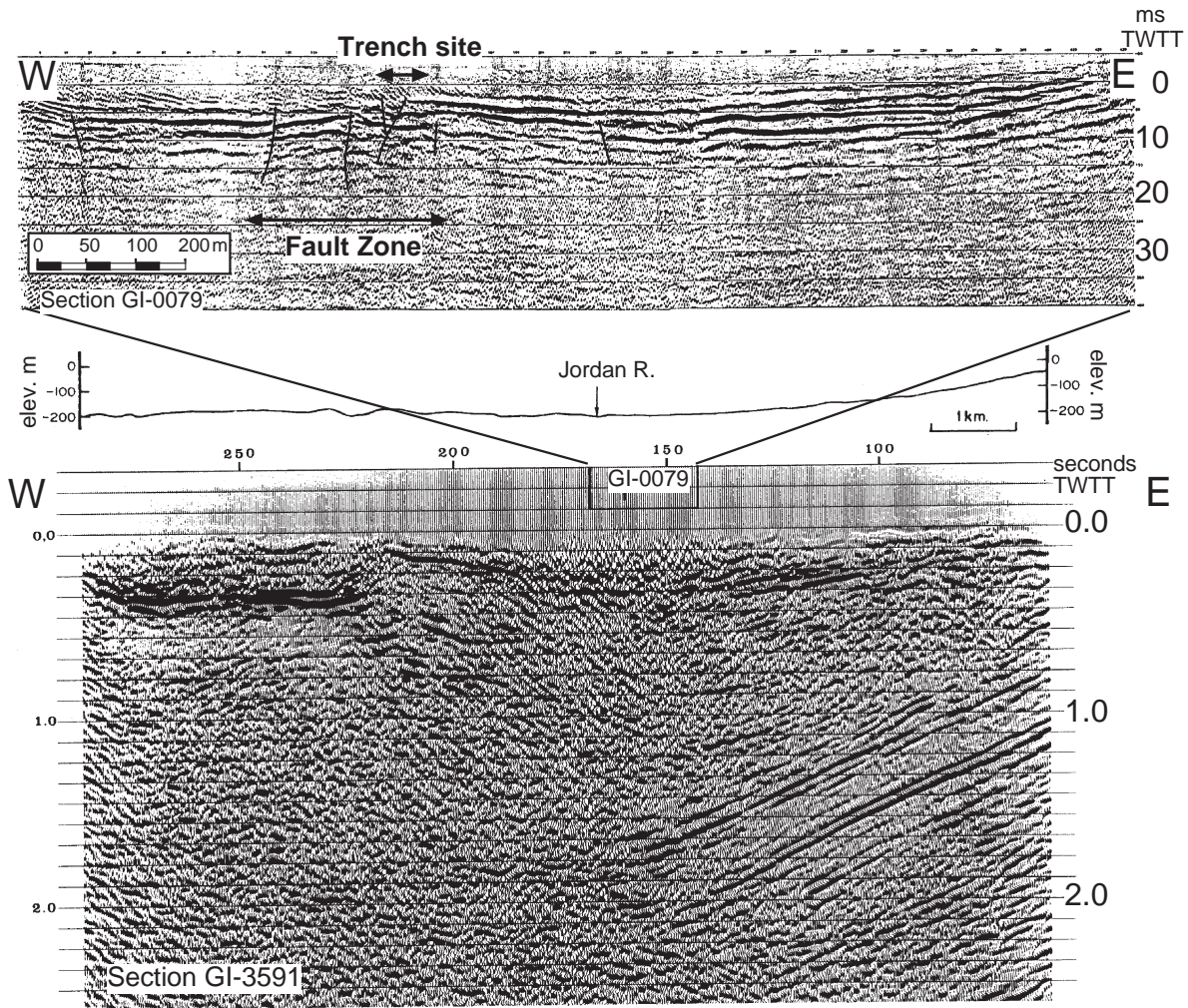


Fig. 3. Bottom: a deep seismic time-section showing clear continuous, west-dipping reflectors on the east, which terminate abruptly at the fault zone (reproduced from [15]). Both the source and the receiver interval is 2.5 m. Top: an E–W high-resolution seismic reflection time-section showing the fault zone in the form of offset reflectors. The uppermost reflectors are faulted within a ~350-m-wide zone. The reflectors are probably Pliocene flood basalts, which outcrop about 500 m to the west.

that its margins are between T1 and T3. Therefore we traced the margins of the sand in a series of fault-parallel trenches on both sides of the fault.

We ended up excavating a total of 25 trenches across and parallel to the fault over a period of 3 years. The northern trenches revealed a set of displaced nested-channels below the unfaulted present stream. In the southern trenches we exposed a single displaced channel. The fault zone, which is less than 1 m wide, is very clear (Fig. 5). It is the data collected from these excavations (Figs. 5–9 and Tables 1 and 2)

that we use to reconstruct the earthquake history of the northern Bet-Zayda Valley.

3. Stratigraphy at Bet-Zayda

The Bet-Zayda site is located on the delta of the Jordan River, where it discharges into the Sea of Galilee (Kinneret) at 208–207 m below mean sea level. Consequently, the stratigraphy reflects this depositional environment. The Bet-Zayda Valley is

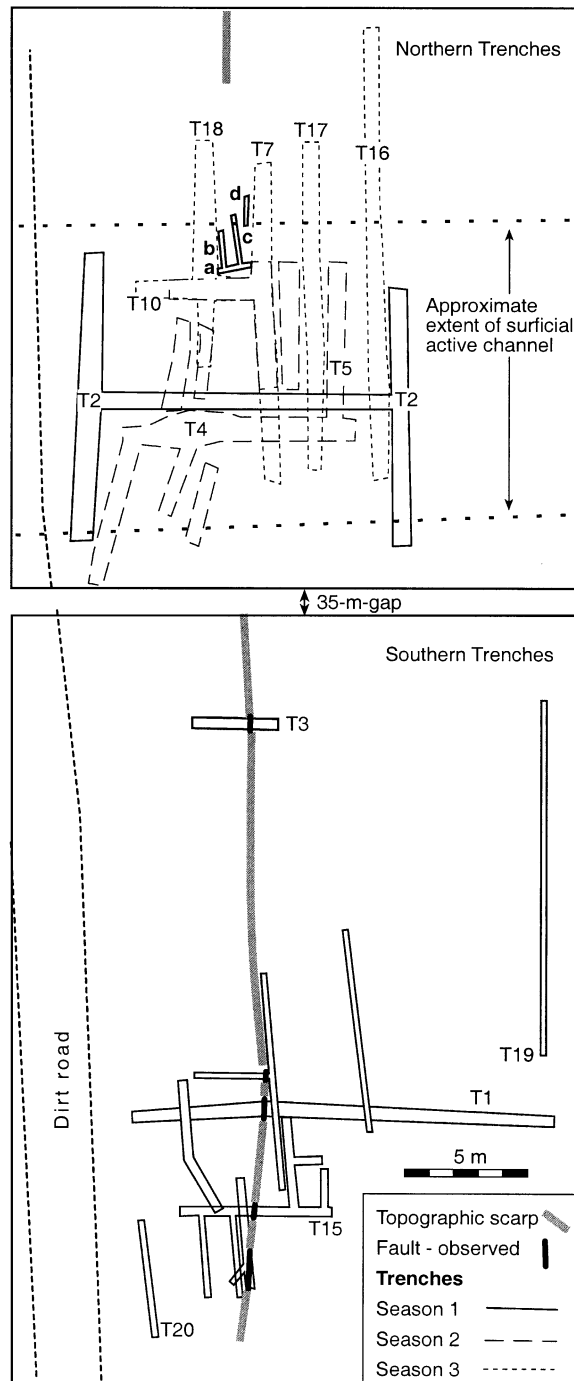


Fig. 4. Map of trench site. The site was developed over three seasons, each marked with a different line.

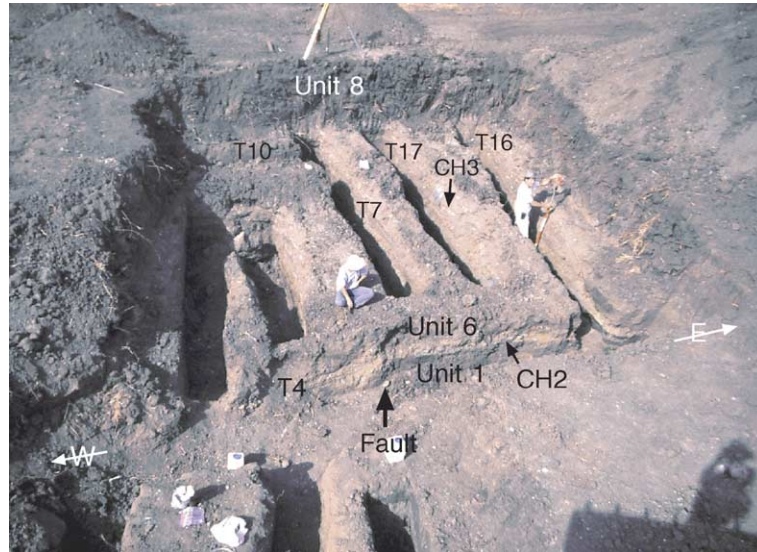


Fig. 5. A general view of the northern trench site in the second season. Trench T4 crosses the fault (arrow), which truncates Unit 1 and the pebble layer of CH2 (see log on Fig. 7). The stream channels are commonly light-coloured whereas the lacustrine clay of units 1 and 8 is dark.

flooded only during extreme high stands. For example water levels during the 20th century were -214 m and -208 m, but in “normal” years they fluctuated between -211 in the autumn and -209 in the spring [16].

The exposed sediments represent basically three different types of deposition: (1) massive clays, which we interpret as lacustrine in nature; (2) fossiliferous, foreset-bedded gravelly sand that is limited to channels and is interpreted as estuarine and deltaic distributary channel alluvium; and (3) pebbles and coarse sand of channelled fluvial alluvium, which locally may interfinger with distributary channel alluvium. We describe the character, distribution, and age of these deposits below, along with their relationship to the fault (Figs. 5–9).

Unit 1 is a deposit of dark stiff clay that underlies the entire area of study. Locally, the colour of this clayey deposit was greenish-bluish grey when trenches were first opened, but rapidly oxidized to a grey hue after a few days. The clay was found to be generally massive, without any recognizable stratigraphy, possibly due to bioturbation. Based on its fine texture, we infer a lacustrine origin for the clay unit, indicating high stand of Lake Kinneret. Unit 1a consists of sandy clay, which appears irregularly, possibly attesting to lens-like distribution. A series of stream channels that represent deposition and lateral migration over some period of time is denoted as

CH1–CH5. CH1 appears only in the southern trenches. The oldest and deepest channel in the northern trenches, unit CH2, contains a conglomerate of up to fist-size pebbles, devoid of fossils. We interpret this to be a fluvial channel incised into the previously deposited lake clays of unit 1. CH2 is overlain by fine to coarse sand. In some exposures, the sand is stratified, with foreset beds defining much of the stratigraphy. Thus the channels of units CH2 through CH5 must have been deposited during a period of relative low lake-level when base-level lowering would have forced incision of distributary channels, somewhat similar to the present state.

Unit CH3 flowed across the fault a few meters north of CH2, almost at the same level. The relative age of the two channels is based on on-lapping relationships in trenches T16, T17, and T7, where the southern margins of CH3 lay on top of CH2 (Fig. 6). Incised into the channel CH3 deposit and into the basal clay is channel CH4. CH4 deposits are locally stratified, with foreset-bedded sandy gravel interbedded or channelled with more massive gravelly alluvium. An associated fine-grained cap of clayey alluvium apparently represents deposition in a quite water environment after channel abandonment. These gravels are also generally devoid of fossils so we interpret these channels as primarily fluvial in nature. CH4 is thin on the east in trenches T16, T17, and T7

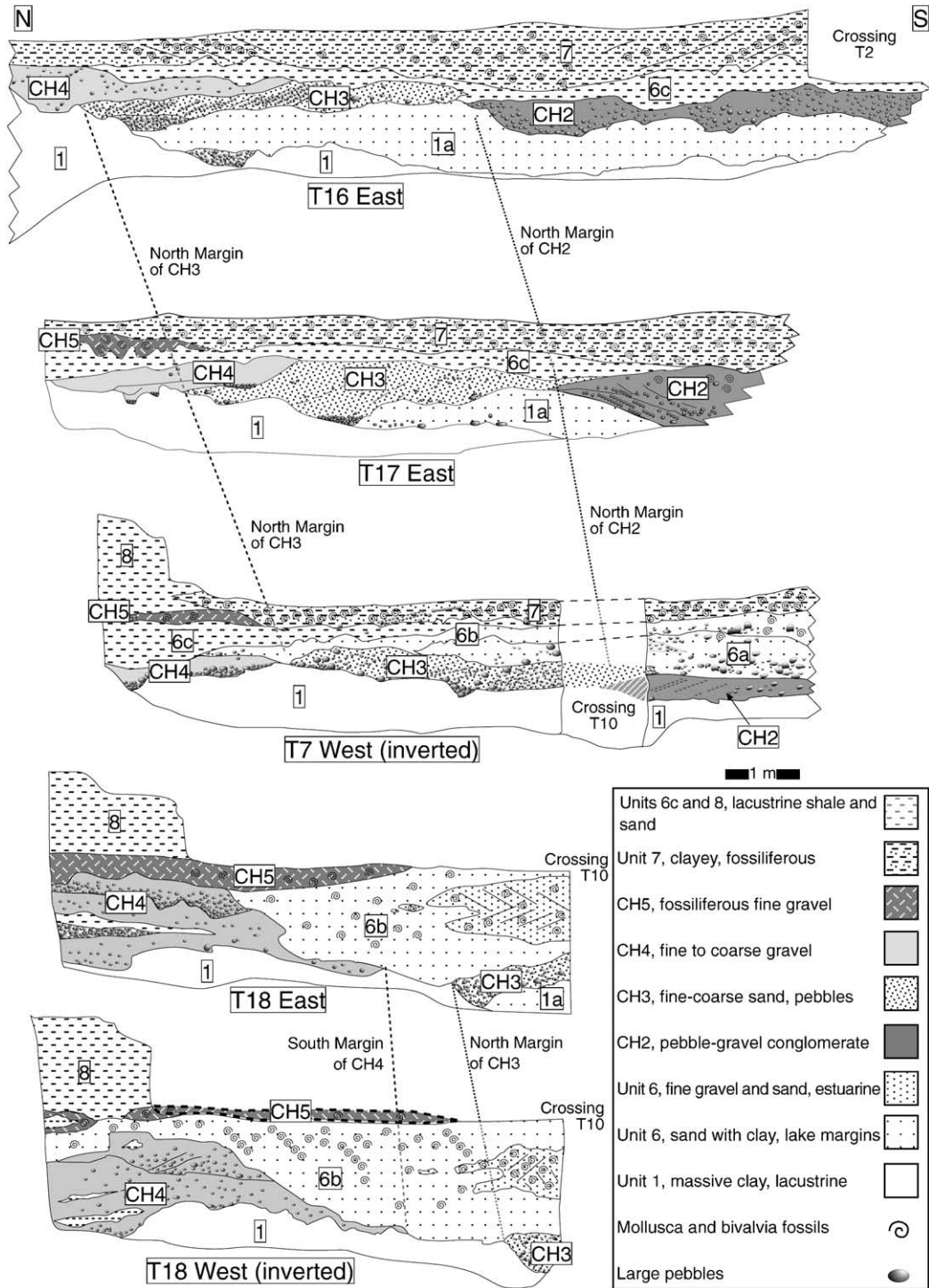


Fig. 6. Fault-parallel trench logs of the northern group show offset stream channels. Alternating alluvium and lake deposits reflect fluctuations of water level of the Kinneret. Clay units 1 and 8 below and above the channels indicate high stands of the Kinneret whereas channel incision indicates low stand.

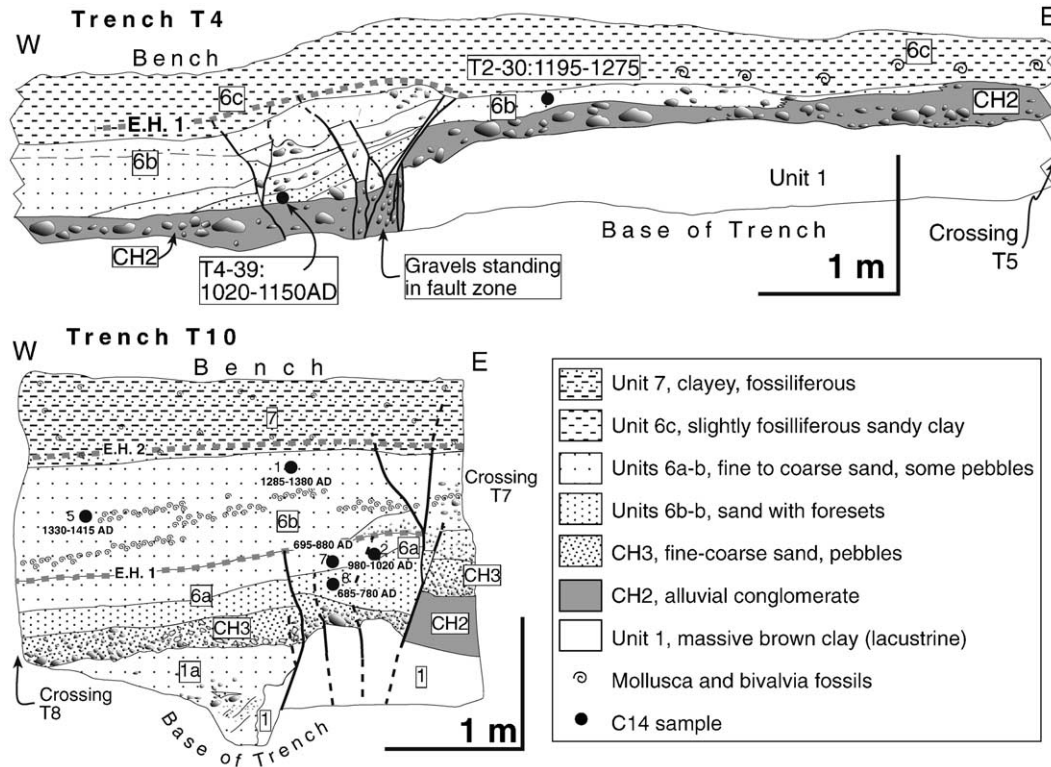


Fig. 7. Trench logs and dated stratigraphy of Trenches T10 (top) and T4 (bottom). Solid lines mark the faults, dashed are very faint, discontinuous disturbances, which we attribute to late adjustments of the overlying strata. Two slip events are observed in T10. Based only on the C14 dating, the first slip event (E.H. 1) postdates the 12th century and predates the 13th century. The second slip (E.H. 2) postdates the 15th century. Based on historical earthquake catalogues and correlation to Ateret we correlated the slip events to the earthquakes of 20 May, 1202 and 30 October 1759. The trace of the 1759 slip is not clear in trench T7 because of the poorly-consolidated unit 6c. We therefore mark only E.H. 1.

but widens and becomes thicker and about half a meter deeper in T18, forming a small fan upon crossing the fault to the west. We interpret this change as an indication for a small scarp of about 0.5 m.

Unit 6 is variable, and we divide it into three different facies denoted 6a–c, which show irregular shapes, perhaps reflecting shifting streams and erosion. Unit 6a, which appears in trench T7 is made of fine gravel and some pebbles, with scattered, mostly broken and fragmented fossils. Unit 6b is fossiliferous sandy gravel, but no pebbles. The fossiliferous nature of this alluvium suggests that it was deposited in a low energy distributary channel environment. Unit 6c is sandy clay with scarce fossils, which disappears toward west and is absent in trench T18. Units 6b and 6c lay on top of CH4 but farther west unit 6b interfingers with it. On the eastern wall of T18 CH4 is overlain by channel CH5, which was truncated before units 6b and 6c were

deposited. The irregular appearance of units 6a–c probably reflects meanders of the palaeochannel, therefore we do not use them to measure slip.

Unit CH5 is a gravel-filled, southwest-trending channel. Its southern margin, which is exposed in the large trenches and in small ones (20-cm-wide) excavated very close to the fault (denoted a–d on Figs 4 and 10), is displaced by 0.5 m, the same as CH4. The northern margins of this channel are not exposed in the trenches. Channel CH5 can be interpreted as conformable with the underlying unit 6, but it locally truncates the bedding of unit CH4 as seen in trench T18 East. A distinct difference between CH5 and the older channels CH3 and CH4 are the presence of numerous mollusc shells stratified within the younger deposit. This observation suggests a return to deltaic distributary channel deposition, or even estuarine, probably suggesting a slight rise in lake level.

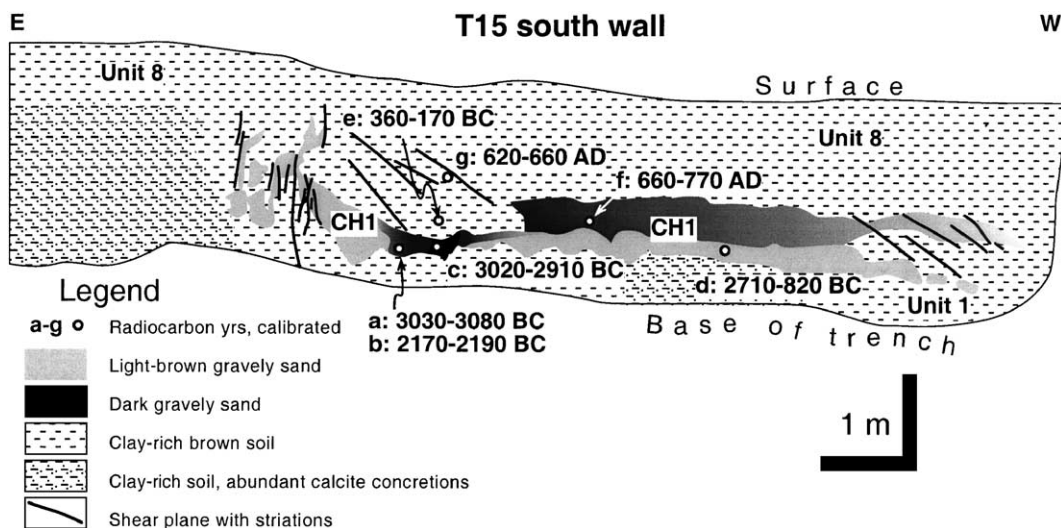


Fig. 8. The stratigraphy near the fault at Trench T15 of the southern group. The oldest age of bulk organic matter leached from of the alluvial sand layer is $5 \text{ ka} \pm 50 \text{ yr}$. The concordance of the other dates with the stratigraphy indicate their reliability. The top of the trench shows the surface expression of the fault, where the eastern side is about 0.8 m higher than the western side.

The sandy clay of unit 6c grades upward into clayey, fossiliferous alluvium, which we designate as unit 7. Without the fossils, unit 7 would look very similar to the clayey alluvium of unit 6c. Consequently, we interpret them to have been deposited in a similar depositional environment. Thus, it appears that the increase in lake level indicated by the shale deposits of unit 6c and the fossils in unit CH5 has persisted through the deposition of unit 7.

Unit 8 is a generally massive, dark, organic-rich clayey deposit, capped at the surface by a soil layer. This unit, which forms the surface of most of the study area, is commonly up to 1.5 m thick, composed of massive, dark brown clay, devoid of stratification. No fossils were found, but a few shards of ceramics were encountered, unfortunately too small to identify. The soil's uppermost ~50 cm is ploughed. Roots are abundant.

The stratigraphy in the southern group of trenches is much simpler than the northern group (Fig. 8). The same basal massive dark clay of unit 1 is found there too. A variegated layer of alluvial coarse sand with no fossils in it was found in the form of a stream channel. The alluvial sand is overlain by a massive dark-brown clayey soil whose thickness is 1.5 m on the eastern side of the fault and about 3 m west of it. We correlate it with unit 8 of the northern trenches. The transition between unit 1 below the

sand and unit 8 above it is gradual whereas the contacts with the sand are mostly sharp. Abundant calcite concretions characterize the area east of the fault as well as some places below the sand layers. The trench map view reveals that the northern margin of the stream is offset by 15 m by the fault and the southern margin is offset by 9 m.

4. C14 dating

We collected all the detrital charcoal that was encountered in the trenches. The samples were dated in the Kimmel Center of the Weizmann Institute using conventional alpha counting. Small samples were measured by Atomic Mass Spectroscopy. The possibility to date the shells was considered but since the systematics of C14 in this environment is unknown, in particular the reservoir time, we decided to examine this option in a separate study. Age data are summarised in Fig. 9 and Table 1.

Trench T10 (Fig. 7), which cut the fault zone within the northern trenches, yielded a few indicative ages corresponding to two groups of faults. The earlier group offsets the stratigraphic units from which C14 ages range from 720–770 AD to 980–1020 AD. These faults terminate upward at unit 6b, in which C14 ages are from 1285–1380 AD to 1330–1415 AD.

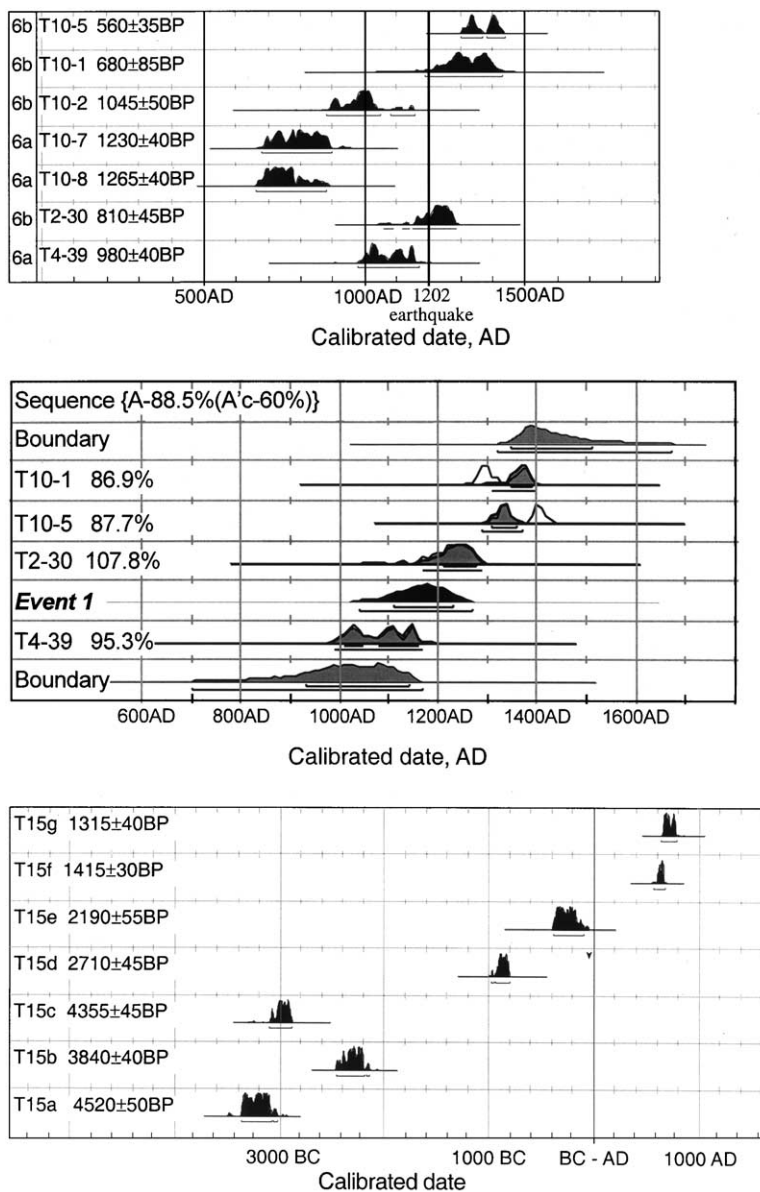


Fig. 9. Top: calibrated date distribution for samples from trenches T2, T4, and T10. Center: probability density functions for radiocarbon dates that constrain the timing of the penultimate event at the Bet-Zayda palaeoseismic site. The dates were trimmed with Bayesian statistics in OxCal, and the probability density function for the event age is calculated from the radiocarbon ages. Note that the historical 1202 earthquake falls within the probability distribution, and is in fact the only historical earthquake in the vicinity that can possibly fit the age distribution. This indicates that the detrital charcoal dated for this study was not resident in the system for an extended period of time (decades versus centuries). Bottom: calibrated date distribution for samples from trench T15. Calibration of C14 ages was done with the Bronk Ramsey's (2002) OxCal program version 3.8 using the atmospheric data of Stuiver et al. [48].

The second group of faults offsets unit 6b and the lower part of Unit 7. Hence, the first faulting is constrained between 1020 AD and 1280 AD. Two C14 dates in trench T4 also show that the first faulting

is constrained between 1020–1150 AD and 1195–1275 AD (Fig. 7). Based on the historical earthquake record and the observations at Ateret [3] the first slip event can be correlated to the historical earthquake of

Table 1
C14 dates used for constraining the time of earthquakes that ruptured the surface at Bet-Zayda

Sample ID	Lab#	Type	Unit	Stratig	¹⁴ C Age	±	Calibrated age 2σ	δ ¹³ C PDB
T10-1	3299	Charcoal	6b	Post E1, pre E2	680	85	AD 1285–1380	–25
T10-5	3298	Charcoal	6b	Post E1, pre E2	560	35	AD 1330–1415	–26.15
T2-30	3294	Charcoal	6b	Post E1, pre E2	810	45	AD 1195–1275	Lost
T10-2	3293	Charcoal	6a	Pre E1	1045	50	AD 980–1020	–25.4
T10-7	3304	Charcoal	6a	Pre E1	1230	40	AD 695–880	–24.1
T10-8	3290	Sediment	6a	Pre E1	1265	40	AD 685–780	Small
T4-39	3303	Charcoal	6a	Pre E1	980	40	AD 1020–1150	–25.4
T15a	76819	Sediment			4520	50	BC 3030–3080	–25
T15b	76327	Sediment			3840	40	BC 2170–2190	–27
T15c	3546	Sediment			4355	45	BC 3020–2910	–33.1
T15d	3547	Sediment			2710	45	BC 2710–820	–24.9
T15e	3548	Sediment			2190	55	BC 360–170	–23.1
T15f	3550	Sediment			1415	30	AD 620–660	–18.5
T15g	3551	Sediment			1315	40	AD 660–770	–24

The material dated in the sediment samples was the residue of acid–base–acid treated bulk sediment. Sample T15b is humic acid (base-soluble humic extract from sediments, re-precipitated with strong acid). Stratigraphic position refers to the earthquake of 1202 as E1 and to the earthquake of 1759 as E2.

May 20, 1202. The time of the second event has only a lower bound—it postdates 1415 AD. In Fig. 9 we present probability density functions for the radiocarbon dates that constrain the timing of the penultimate event at Bet-Zayda. The historical 1202 earthquake falls within the probability distribution, and is in fact the only historical earthquake in the vicinity that can possibly fit the age distribution. This indicates that the detrital charcoal dated for this study was not resident in the system for an extended period of time (decades versus centuries).

In the southern trenches we did not find any charcoal. We therefore dated the disseminated organic matter and carbonate concretions extracted from the sediment by dissolving all the carbonate material in the samples. The earliest age of the distinct sand unit was determined to 5 ka ±50 yr and the youngest age in it is about 700 AD ±50 yr (Fig. 8; Table 1). All C14 ages from trench T15 but one are in agreement with the stratigraphy. This agreement indicates that

the organic matter in the clay unit has been stable since deposition and no major re-distribution occurred. One sample of humic acid, T15b is younger than the organic residue samples T15c and T15a from the same level.

5. Slip in the Northern Trenches

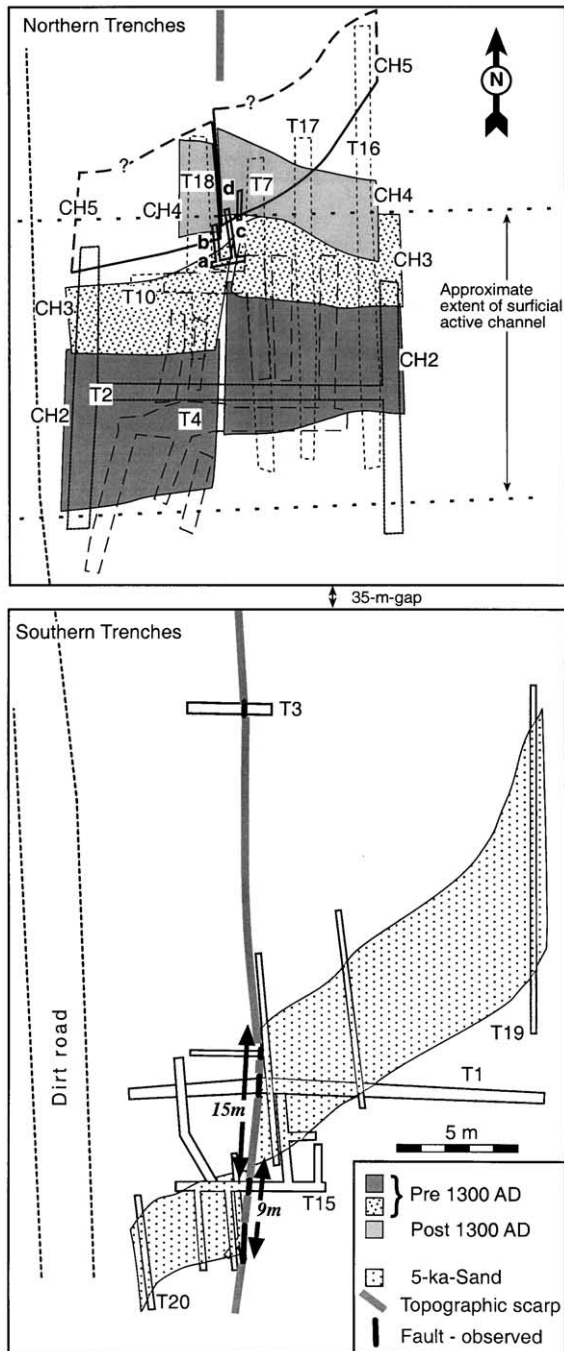
The linear channels CH2–CH5 (Fig. 6), which cut across the fault, provide the piercing points for measuring slip. The southern margins of both CH2 and CH3 are offset 2.7 ± 0.2 m measured less than 0.5 m from the fault (Fig. 10). The northern margin of CH3 shows a sigmoid shape, which we interpret as the result of erosion of the opposing corner by the west-flowing stream soon after slip occurred. Measured about 2 m away from the fault the offset is exactly the same as the southern margins, 2.7 ± 0.3 m. The margins of the younger channel CH4 are offset

Table 2
Offset stream channels that are used as slip markers in Bet-Zayda (ages marked on Figs. 7 and 8)

Unit	Lithology	Age	Offset (m)	±
CH1	Coarse sand	5000 yr bp	15	0.2
CH2	Pebbles	Pre 685AD	2.7	0.1
CH3	Pebbles in coarse sand	Pre 685AD	2.7	0.1
CH4	Pebbles in coarse sand	Post earthquake E1, pre earthquake E2	0.5	0.05
CH5	Pebbles in coarse sand	Post earthquake E1, pre earthquake E2	0.5	0.05

0.5 ± 0.1 m. The southern margin of the youngest buried channel, CH5, shows 0.5 m offset. We did not reach the northern margin of this channel. We interpret the offset channels as showing two slip

events. The first 2.2 ± 0.3 m postdates CH2 and CH3 and predates CH4 and CH5. Additional 0.5 ± 0.1 m postdates CH5. The active stream at the surface is not faulted (Fig. 2).



6. Slip in the Southern Trenches

The first E-striking trench T1 was excavated where the scarp is at its maximum height in order to expose the fault plane. The section on the eastern side of the trench includes four units: massive dark brown clay with carbonate concretions at the bottom, a layer of sandy soil, made of clay and coarse sand of less than 0.5-cm-grains, another layer of dark brown clay, very similar to the one at the bottom, and an uppermost half meter of clayey soil that has been ploughed and is heavily bioturbated. A vertical fault plane was identified at the middle of the trench, characterized by densely spaced shear planes (Fig. 8). The sandy soil layer is truncated by the fault and the section on its western (downthrown) side includes only massive dark-brown clayey soil with carbonate concretions. The fault is recognizable almost up to the surface. The soil in the 2–3 m adjacent to the fault is significantly darker due to high content of organic matter. The dark soil possibly formed in sag ponds, which were rapidly buried at the base of the fault scarp. The only clue for significant horizontal slip in Trenches T1 and T15 is the steepness of the fault plane. The array of southern trenches, which were aimed at tracing the sand's margins enables the resolution of the horizontal and vertical components of the slip to 15 m and 1.2 m respectively. In Trench T15 the sand layer appears only in the western downthrown side. By connecting the sand margins in the trenches on a map (Fig. 10)

Fig. 10. Reconstruction of stream channels. Top: two channels in the northern group of trenches, CH2 and CH3, which postdate C14 dated layers of up to about 12th century AD and predate layers of 13th century AD, are offset 2.7 ± 0.1 m. The 0.5-m-offset of two younger channels, CH4 and CH5, was constrained the offset by digging 20-cm-wide trenches, marked a–d, very close to the fault. Bottom: the distribution of a single layer of alluvial sand in the southern trenches can be interpolated to show an offset channel. The offset of the northern margin of the oldest channel, CH1, which is dated at $5 \text{ ka} \pm 50 \text{ yr}$, is 15 ± 0.2 m. Its southern margin is displaced only 9 m. We explain the difference by erosion of the opposing corner.

we realized that the northern margin is offset sinistrally 15 m and the southern margin is offset 9 m. We attribute the smaller offset to erosion of the corner that opposed the flow after slip events. The C14 ages of the sand layer, the oldest of which is 3030–3080 BC provide a mean slip rate of 3 mm/yr for this fault strand. The absence of detailed stratigraphy does not allow resolution of single ruptures.

7. Discussion

7.1. Candidate earthquakes

The faulting in the northern trenches postdates the carbon dates of 1200 AD (Fig. 7). We consider earthquakes that were reported to have caused damage in northern Israel and Jordan, southern Lebanon, and SW Syria as candidates for being associated with slip at the Bet-Zayda. Catalogues of historical earthquakes [17, 18] list the earthquakes of 1837, 1546, 1759, and 1202. The 20 May 1202 event displaced the walls of the Crusader fortress of Ateret by 1.6 m [3]. Its estimated zone of damage to buildings (meisoseismal zone) extends from ~90 km south to ~160 km north of the Bet-Zayda. It was felt in the entire eastern Mediterranean region and throughout the Levant. The magnitude was estimated at 7.6, with maximum displacement of about 2.5 m [19].

The 1546 earthquake was considered strong [18], but we accept Ambraseys and Karcz's analysis [20] that shows grossly exaggerated reporting and concludes that it was a medium-size earthquake, which caused minor damage in the Judea.

Two close events occurred on 30 October and 25 November 1759. Sieberg [21] located the maximum damage zone of the October earthquake between the Sea of Galilee and the Hula Valley, and that of the November event some 150 km farther north in northeast Lebanon. Ambraseys and Barazangi [22] quote a letter dated 1760 in which the French ambassador to Beirut reports surface ruptures along 100 km of the Yammuneh segment of the Dead Sea Transform and attributes them to the November 1759 earthquake. They estimate the magnitude of the 25 November 1759 earthquake at ~7.4. The October 1759 M ~6.6 foreshock, determined on the basis of isoseismals that centre at the Jordan Gorge [21,22],

could be related to faulting along the Jordan Gorge, at Ateret as well as at Bet-Zayda.

The most recent destructive earthquake to strike the study area was the 1 January 1837 Safed earthquake. The severe damage in Safed and Tiberias, IX–X Mercalli intensity probably biased Vered and Striem to draw isoseismals that centre at the Jordan Gorge [23]. However, using previously unavailable additional data to re-evaluate the meisoseismal zone led to the conclusion that it was an M 7, probably a multiple event, which ruptured the Hula–Roum fault [24]. We accept the latter analysis and assume that the 1837 earthquake did not rupture the fault at Bet-Zayda. Hence the most probable ruptures observed in the northern trenches at Bet-Zayda are associated with the 20 May 1202 and 30 October 1759 earthquakes.

An important observation can be made regarding the reliability of historical accounts. We note that the centre of damage in the crude isoseismal maps [21], which are based on data available in the early 20th century, is confirmed by our studies along the Jordan Gorge. It seems that earthquakes that are well documented by contemporaries can be characterized fairly reliably in terms of the maximum damage zone, from which the magnitude and rupture segment can be roughly estimated.

The trenches prove that N-striking topographic step crossing the otherwise flat Bet-Zayda valley is definitely a fault-related scarp. The presence of the scarp in spite of ploughing, occasional inundation of the Valley by the Sea of Galilee, and the sediments brought by the Jordan River and smaller streams from the Golan Heights require its recent renewal.

The locations and amount of slip, which we observe in the trenches, are in agreement with previous estimates of the earthquake magnitudes based on the extent of damage [19,22]. However the available data are not sufficient yet to constrain the length of the ruptures. Based on empirical relations, (e.g., [25,26]) the ~M7.6 1202 earthquake may have ruptured about 100 km long fault, and the October 1759 earthquake may have ruptured about 15–20 km. Therefore we expect to find different palaeoseismic record on the southern side of the Sea of Galilee at least for a few earthquake cycles, somewhat similar to the behaviour of the North Anatolian Fault in the 20th century [27].

In the southern trenches we recognize an older single slip marker in the form of alluvial sand layer,

confined laterally with margins showing a sand-to-clay transition typically over less than 0.5 m. The northern margin is offset left-laterally 15 m and the southern margin is offset only 9 m. This difference can be explained if the stream incised into the scarp and truncated the corners that formed as the southern margin moved northward on the eastern side during slip events. This process of ‘smoothing’ the southern margin went on for some time during which the fault slipped 6 m. After the channel was abandoned and became inactive, it was buried by lacustrine clay and subsequent 9 m of slip took place. The total slip is therefore 15 m on the north and only 9 m on the south. We are unable to separate the total of 15 m into individual slip events. The mean slip rate is 3 mm/yr for the last 5 kyr or 12.3 m in 3800 years prior to the 1202 event, i.e., 3.2 mm/yr. We do not see any other fault strand at the surface in the Bet-Zayda Valley but this possibility cannot be excluded because the seismic reflection shows several strands in the fault zone (Fig. 3). Hence the 3 mm/yr slip rate is a minimum for the DST. Other slip rate estimates vary between less than 1 mm/yr and 20 mm/yr (Table 3). Estimates based on palaeoseismic data from the Arava Valley south of the Dead Sea are just slightly higher than 3 mm/yr and can be considered in agreement with our result. However palaeoseismic data in the northern part of the DST suggest a slip rate of 7 mm/yr in the late Holocene [5]. One possible reason for these apparent discrepancies might be the different time windows and different fault segments examined in the various studies. Temporal and spatial clustering of earthquakes may lead to estimations of slip rates that do not represent the long-term behaviour of faults [28]. Our best estimate for the Holocene is 4 ± 1 mm/yr.

The long-term slip on the rate DST, assuming the total 105 km of slip postdates the emplacement of 20–19 Ma dikes in Sinai and Arabia is about 5 mm/yr [29]. Our Holocene slip rate value may be lower either due to insufficient sampling (missed parallel segments) or some aseismic slip, or due to slowing of the plate movements. Garfunkel et al. [30] estimated that the seismic slip during historical earthquakes accounts for about one-third of the long-term geologic slip. The new data reduce the discrepancy but do not eliminate it. The current low level of microseismic activity along the DST probably indicates that it behaves in a

Table 3
Slip rate estimates of the Dead Sea Fault

Period	Rate (mm/yr)	Data	Reference
Late Pleistocene–Recent	10	Geological	[34]
Last 1000 yr	0.8–1.7	Historical	[30]
Plio–Pleistocene	7–10	Geological	[30]
Last 4500 yr	2.2	Seismicity	[35]
Late Pleistocene	6.4 ± 0.4	Seismicity	[36]
Plio–Pleistocene	6	Plate kinematics	[37]
	($0.283^\circ/\text{ma}$)		
Holocene	9	Geological	[38]
Plio–Pleistocene	20	Geological	[39]
Holocene	>0.7	Geological	[40]
Plio–Pleistocene	5.4–6.1	Geological	[41]
Plio–Pleistocene	3–7	Drainage systems, Arava Fault	[42]
Pleistocene	2–6, prefer 4	Alluvial fans, N. Arava	[4]
Pleistocene	4.7 ± 1.3	Alluvial fans, Arava	[6]
Last 2000 yr	6.9 ± 0.1	Paleo and Archaeoseismology, Missyaf (DSF in Syria)	[5]
1996–1999	2.6 ± 1	Geodesy, GPS	[43]
1996–2003	3.3 ± 0.4	Geodesy, GPS	[32]
25 ka	3.8–6.4	Geological, Lebanon	[44]
Last 5000 yr	≥ 3	Stream channel, Jordan Gorge	This study

stick–slip manner, although a-seismic motion (creep or silent earthquakes) cannot be precluded. To resolve this problem we need to know the detailed geometry of the fault zone and the slip on all parallel fault strands, impose tighter constraint on the time of DST initiation, and acquire geodetic measurements on both sides of the fault.

8. Conclusions

Three-dimensional trenching proved to be a successful method in the Bet-Zayda Valley. Our study demonstrates how a palaeoseismic investigation is complemented by archaeological and historical data to characterize the seismic activity along the northern DST. We conclude that the JGF has been the main active strand of the DST during Late Holocene. Other normal faults have been also active in the Plio–Pleistocene, keeping up with, and even exceeding sediment accumulation in the basin. The Late Holocene motion on the JGF has been primarily strike–

slip (15 m); vertical component is only 1.2 m. A similar proportion is estimated between the total 100 km slip on the DST and the thickness of the fill in the Dead Sea Basin [31]. Our observations confirm the plate tectonics paradigm of sinistral slip between the Arabia and Sinai. C14 dating of bulk organic matter constrain the minimum age of the layer that is offset by 15 m to 5 kyr, yielding a minimum average Late Holocene slip rate of 3 mm/yr. This rate is of the same order of the model based on GPS geodesy [32] and results of palaeoseismic studies south of the Dead Sea [4,6] but the rate during the last two millennia further north is more than double [5]. Our observations establish the last two earthquakes at the Jordan Gorge fault segment occurred on May 20 1202 and October 30 1759. They were associated with significantly different amount of rupture, 2.2 ± 0.2 m in the 1202 earthquake and 0.5 ± 0.1 m in the 1759 earthquake. Along-strike variation of slip is apparent for the 1202 event, which offset only 1.6 m at the Ateret site, 12 km north of the Bet-Zayda Valley. The 1759 slip is the same at both sites. This result is incompatible with the “characteristic earthquake” model [33]. The independent analyses of the damage inflicted by the 1202 and 1759 earthquakes [19,21,22] yielded a correct estimate of the location and magnitude of the ruptures. We believe that historical earthquakes that were relatively well documented can be characterized quite reliably in terms of their locations and magnitudes by careful analysis of historical reports.

Acknowledgments

We thank our colleagues Rivka Amit, Ezra Zilberman, Daniel Wachs, Yariv Hami’el, Yuval Bartov, Revital Ken-Tor, Dany Gluck, Yonni Shaked, Meir Abelson, and Ari Matmon for constructive advice and assistance in the fieldwork. Technical assistance by Dany Ergas, Shlomo Ashkenazy, Moshe Arnon, Ya’akov Mizrahi is greatly appreciated. We are also grateful to the farmers of Almagor for their hospitality and for allowing us to work in their fields, in particular Avi Bental and Avishai. Elisabeta Boaretto is thanked for performing C14 analyses and discussing their implications. Gordon Seitz is thanked for contributing C14 analyses. We are thankful to Mustapha Meghraoui and an anonymous referee for

constructive reviews. The study was funded by the Binational Science Foundation Israel–U.S. and the Earth Sciences Administration of the Ministry of Infrastructure of Israel.

References

- [1] R. Freund, I. Zak, Z. Garfunkel, Age and rate of the sinistral movement along the Dead Sea Rift, *Nature* 220 (1968) 253–255.
- [2] A.M. Quennell, Tectonics of the Dead Sea rift, Congreso Geologico Internacional, 20th Sesion, Asociacion de Servicios Geologicos Africanos, Mexico City, 1956, pp. 385–405.
- [3] R. Ellenblum, S. Marco, A. Agnon, T. Rockwell, A. Boas, Crusader castle torn apart by earthquake at dawn, 20 May 1202, *Geology* 26 (1998) 303–306.
- [4] Y. Klinger, J.P. Avouac, N. Abou-Karaki, L. Dorbath, D. Bourles, J.L. Reyss, Slip rate on the Dead Sea transform fault in northern Araba Valley (Jordan), *Geophys. J. Int.* 142 (2000) 755–768.
- [5] M. Meghraoui, F. Gomez, R. Sbeinati, J.V. derWoerd, M. Mouty, A.N. Darkal, Y. Radwan, I. Layyous, H.A. Najjar, R. Darawcheh, F. Hijazi, R. Al-Ghazzi, M. Barazangi, Evidence for 830 years of seismic quiescence from palaeoseismology, archaeoseismology and historical seismicity along the Dead Sea fault in Syria, *Earth Planet. Sci. Lett.* 210 (2003) 35–52.
- [6] T.M. Niemi, H. Zhang, M. Atallah, B.J. Harrison, Late Pleistocene and Holocene slip rate of the Northern Wadi Araba fault, Dead Sea Transform, Jordan, *J. Seismol.* 5 (2001) 449–474.
- [7] Y. Klinger, L. Rivera, H. Haessler, J.C. Maurin, Active faulting in the Gulf of Aqaba: new knowledge from the Mw7.3 earthquake of 22 November 1995, *Bull. Seismol. Soc. Am.* 89 (1999) 1025–1036.
- [8] A. Salamon, Seismotectonic Analysis of Earthquakes in Israel and Adjacent Areas, PhD, The Hebrew University of Jerusalem, 1993.
- [9] G. Shamir, G. Baer, A. Hofstetter, Three-dimensional elastic earthquake modelling based on integrated seismological and InSAR data: the Mw=7.2 Nuweiba earthquake, gulf of Elat/Aqaba 1995 November, *Geophys. J. Int.* 154 (2003) 731–744.
- [10] S. Marco, A. Agnon, R. Ellenblum, A. Eidelman, U. Basson, A. Boas, 817-year-old walls offset sinistrally 2.1 m by the Dead Sea Transform, Israel, *J. Geodyn.* 24 (1997) 11–20.
- [11] Z. Ben-Avraham, U. ten-Brink, R. Bell, M. Reznikov, Gravity field over the Sea of Galilee: evidence for a composite basin along a transform fault, *J. Geophys. Res.* 101 (1996) 533–544.
- [12] S. Hurwitz, Z. Garfunkel, Y. Ben-Gai, M. Reznikov, Y. Rotstein, H. Gvirtzman, The tectonic framework of a complex pull-apart basin: seismic reflection observations in the Sea of Galilee, Dead Sea transform, *Tectonophysics* 359 (2002) 289–306.
- [13] L. Eppelbaum, Z. Ben-Avraham, Y. Katz, S. Marco, Sea of Galilee: comprehensive analysis of magnetic anomalies, *Isr. J. Earth-Sci.* 53 (2004) 151–171.

- [14] A. Zurieli, Z. Ben-Avraham, S. Marco, Y. Ben-Gai, Neotectonics in Kinarot Valley based on high-resolution seismic reflection, in: A. Beck, Y. Katz, R. Ken-Tor (Eds.), Israel Geological Society Annual Meeting, Ma'agan, 2002, p. 137.
- [15] Y. Rotstein, Y. Bartov, Seismic reflection across a continental transform: an example from a convergent segment of the Dead Sea rift, *J. Geophys. Res.* 94 (1989) 2902–2912.
- [16] K.D. Hambright, T. Zohary, W. Eckert, Potential influence of low water levels on Lake Kinneret: re-appraisal and modification of early hypotheses, *Limnologia* 27 (1997) 149–155.
- [17] N.N. Ambraseys, C.P. Melville, R.D. Adams, *The Seismicity of Egypt, Arabia, and the Red Sea: A Historical Review*, Cambridge University Press, Cambridge, 1994, 181 pp.
- [18] D.H.K. Amiran, E. Arieh, T. Turcotte, Earthquakes in Israel and adjacent areas: macroseismic observations since 100 B.C.E., *Isr. Explor. J.* 44 (1994) 260–305.
- [19] N.N. Ambraseys, C.P. Melville, An analysis of the eastern Mediterranean earthquake of 20 May 1202, in: W.K.H. Lee, H. Meyers, K. Shimazaki (Eds.), *Historical Seismograms and Earthquakes of the World*, Academic Press, San Diego, CA, 1988, pp. 181–200.
- [20] N. Ambraseys, I. Karcz, The earthquake of 1546 in the Holy Land, *Terra Nova* 4 (1992) 253–262.
- [21] A. Sieberg, *Erdbebengeographie, Handbuch der Geophysik, Band, vol. IV*, Borntraeger, Berlin, 1932, pp. 527–1005.
- [22] N.N. Ambraseys, M. Barazangi, The 1759 earthquake in the Bekaa valley: implications for earthquake hazard assessment in the eastern Mediterranean region, *J. Geophys. Res.* 94 (1989) 4007–4013.
- [23] M. Vered, H.L. Striem, A macroseismic study and the implications of structural damage of two recent major earthquakes in the Jordan rift, *Bull. Seismol. Soc. Am.* 67 (1977) 1607–1613.
- [24] N. Ambraseys, The earthquake of 1 January 1837 in southern Lebanon and northern Israel, *Ann. Geophys.* 40 (1997) 923–935.
- [25] N.N. Ambraseys, J.A. Jackson, Faulting associated with historical and recent earthquakes in the Eastern Mediterranean region, *Geophys. J. Int.* 133 (1998) 390–406.
- [26] D.L. Wells, K.J. Coppersmith, New empirical relationships among magnitudes, rupture length, rupture width, rupture area, and surface displacement, *Bull. Seismol. Soc. Am.* 84 (1994) 974–1002.
- [27] A.A. Barka, K. Kadinsky-Cade, Strike-slip fault geometry in Turkey and its influence on earthquake activity, *Tectonics* 7 (1988) 663–684.
- [28] S. Marco, M. Stein, A. Agnon, H. Ron, Long term earthquake clustering: a 50,000 year paleoseismic record in the Dead Sea Graben, *J. Geophys. Res.* 101 (1996) 6179–6192.
- [29] Y. Bartov, G. Steinitz, M. Eyal, Y. Eyal, Sinistral movement along the Gulf of Aqaba—its age and relation to the opening of the Red Sea, *Nature* 285 (1980) 220–221.
- [30] Z. Garfunkel, I. Zak, R. Freund, Active faulting in the Dead Sea rift, *Tectonophysics* 80 (1981) 1–26.
- [31] A. Ginzburg, Z. Ben-Avraham, A seismic reflection study of the north basin of the dead Sea, Israel, *Geophys. Res. Lett.* 24 (1997) 2063–2066.
- [32] S. Wdowski, Y. Bock, G. Baer, L. Prawirodirdjo, N. Bechor, S. Naaman, R. Knafo, Y. Forrai, Y. Melzer, GPS Measurements of current crustal movements along the Dead Sea Fault, *J. Geophys. Res.* 109 (2004) 1–16.
- [33] D.P. Schwartz, K.J. Coppersmith, Fault behavior and characteristic earthquakes: examples from the Wasach and San andreas fault zones, *J. Geophys. Res.* 89 (1984) 5681–5698.
- [34] G.M. Friedman, Geology and geochemistry of reefs, carbonate sediments and waters, Gulf of Aqaba (Elat), Red Sea, *J. Sediment. Petrol.* 38 (1968) 895–919.
- [35] A. Ben-Menahem, Variation of slip and creep along the Levant Rift over the past 4500 years, *Tectonophysics* 80 (1981) 183–197.
- [36] Z.H. El-Isa, H. Mustafa, Earthquake deformations in the Lisan deposits and seismotectonic implications, *Geophys. J. R. Astron. Soc.* 86 (1986) 413–424.
- [37] S. Joffe, Z. Garfunkel, Plate kinematics of the circum Red Sea—a re-evaluation, *Tectonophysics* 141 (1987) 5–22.
- [38] Z. Reches, D.F. Hoexter, Holocene seismic and tectonic activity in the Dead Sea area, *Tectonophysics* 80 (1981) 235–254.
- [39] G. Steinitz, Y. Bartov, The 1985 time table for the tectonic events along the Dead Sea transform, *Terra Cogn.* 6 (1986) 160.
- [40] M. Gardosh, Z. Reches, Z. Garfunkel, Holocene tectonic deformation along the western margins of the Dead Sea, *Tectonophysics* 180 (1990) 123–137.
- [41] A. Heimann, The Development of the Dead Sea Rift and its Margins in the Northern Israel during the Pliocene and the Pleistocene, *Golan Res. Inst. and Geol. Surv. Isr.*, 1990.
- [42] H. Ginat, Y. Enzel, Y. Avni, Translocation of Plio–Pleistocene drainage system along the Dead Sea Transform, south Israel, *Tectonophysics* 284 (1998) 151–160.
- [43] S. Pe'eri, S. Wdowski, A. Shtibelman, N. Bechor, Current plate motion across the Dead Sea Fault from three years of continuous GPS monitoring, *Geophys. Res. Lett.* 29 (2002). doi:10.1029/2001GL013879.
- [44] M. Daeron, L. Benedetti, P. Tapponnier, A. Surssock, R.C. Finkel, Constraints on the post 25-ka slip rate of the Yammounh fault (Lebanon) using in situ cosmogenic ³⁶Cl dating of offset limestone-clast fans, *Earth Planet. Sci. Lett.* 227 (2004) 105–119.
- [45] Y. Bartov, *Israel-Geological Map 1:500,000, The Survey of Israel*, 1979.
- [46] J.K. Hall, Digital shaded-relief map of Israel and environs 1:500,000, *Geol. Surv. Isr.* (1994).
- [47] Y. Bartov, A. Sneh, L. Fleischer, V. Arad, M. Rosensaft, *Map of Suspect Active Faults in Israel*, The Geological Survey of Israel, Jerusalem, 2002.
- [48] M. Stuiver, P.J. Reimer, E. Bard, J.W. Beck, G.S. Burr, K.A. Hughen, B. Kromer, G. McCormac, J. van-der-Plicht, M. Spurk, INTCAL98 radiocarbon age calibration, 24,000–0 cal BP, *Radiocarbon* 40 (1998) 1041–1083.